

Wave simulation in a 3D coupled numerical and physical wave basin

Z.W. Yang¹, H.B. Bingham², S.X. Liu¹

¹ State Key Laboratory of Coastal and Offshore Engineering, Dalian University of Technology, China

² Department of Mechanical Engineering, Technical University of Denmark

E-mail: ouyangzhiwen@gmail.com, hbb@mek.dtu.dk, liusx@dlut.edu.cn

1. Introduction

The combination of numerical and physical models has increasingly been used for coastal or offshore water wave problems (Gierlevsen et al., 2003; Kofoed-Hansen et al., 2003). This approach allows the numerical model to focus on wave propagation in the offshore region and the physical model to treat the wave transformation in the near-shore region. The primary goal is to exploits the advantages of numerical and physical model to provide an improved description of full-scale, realistic engineering problems. However, the data transfer between the numerical and physical model is only on a stochastic level through bulk parameters, such as the significant wave height and spectral peak frequency.

Zhang et al. (2005, 2007) initially devised an ad hoc unified 3D wave generation theory to deterministically couple the numerical and physical wave basin. This theory accounts for shallow water wave generation theory and dispersive compensates based on the linear assumption. To improve the coupling accuracy, Yang et al. (2013) has extended the exiting model correct to second order, but only for wave flume. A range of stream function simulation tests has confirmed the accuracy and efficiency of this model.

This paper presents recent and preliminary work towards the extension of coupling theory of numerical and physical models to account for 3D coupled wave basin. The derivation of this new model is based on the second-order coupling model (Yang et al., 2013) and the ad hoc unified 3D wave generation theory (Zhang et al., 2007). Using a well-established 3D flexible-order, finite-difference-based fully nonlinear potential flow model (OceanWave 3D) devised by Engsig-Karup et al. (2009) for the numerical wave calculation and a 2D piston-type wavemaker for the physical wave generation, practical applications on unidirectional and multidirectional, regular and irregular, wave cases are presented.

2. Formulation and solution

A Cartesian coordinates (x, y, z) is adopted with xy -plane coincident with the undisturbed free surface and the z -axis directed upwards. The whole simulation domain is divided into a numerical region and a physical region. At the boundary between the two regions, the following condition must be satisfied,

$$U_N(x_0, y, t) = U_P(x_0, y, t) \quad (1-a)$$

$$V_N(x_0, y, t) = V_P(x_0, y, t) \quad (1-b)$$

where, (U_N, V_N) denotes the numerical depth-averaged velocity at x - and y -axis, respectively, which can be obtained from a suitable numerical model, or even any nonlinear wave theory. (U_P, V_P) represent the equivalents for physical model which is mainly used to determine the motion of wave paddle, x_0 the mean position between two models, t the time variable.

Considering the physical region, under the assumption of an inviscid, incompressible fluid undergoing irrotational motion, we can define the velocity potential, $\phi(x, z, t)$. The free-slip condition on the wavemaker reads

$$X_{0t} = \phi_x - \nabla \phi \cdot \nabla X_0 \quad \text{on } x=X_0 \quad (2)$$

where $X_0=X_0(y, z, t)$ is wave paddle position, and ∇ denotes the vertical gradient $\nabla=(\partial y, \partial z)$. The previously defined (ϕ, \tilde{U}, X_0) can be further expanded in a perturbation series as

$$\phi = \varepsilon \phi^{(1)} + \varepsilon^2 \phi^{(2)} + \dots \quad (3-a)$$

$$\tilde{U} = \varepsilon \tilde{U}^{(1)} + \varepsilon^2 \tilde{U}^{(2)} + \dots \quad (3-b)$$

$$X_0 = \varepsilon X_0^{(1)} + \varepsilon^2 X_0^{(2)} + \dots \quad (3-c)$$

where $\tilde{U}=(U, V)$, ε is a small ordering parameter proportional to the wave steepness H/L , with H being the wave height and L the wavelength. Combining Eqs. (2) with (3a) and (3c) yields

$$\varepsilon^1: \quad \phi_x^{(1)} = \frac{\partial X_0^{(1)}(y, t)}{\partial t} \quad (4-a)$$

$$\varepsilon^2: \quad \phi_x^{(2)} + \frac{\partial X_0^{(1)}(y, t)}{\partial y} \phi_y^{(1)} = \frac{\partial X_0^{(2)}(y, t)}{\partial t} \quad (4-b)$$

where we have considered a piston wavemaker such that the wave paddle position is rewritten as $X_0(y, z)$. Applying the shallow water assumption and considering the boundary condition of (1), Eq. (4) can be rewritten as

$$\varepsilon^1: \quad \frac{\partial X_{0,sw}^{(1)}(y, t)}{\partial t} = U_N^{(1)}(X_{0,sw}^{(1)}(y, t), y, t) \quad (5-a)$$

$$\varepsilon^2: \quad \frac{\partial X_{0,sw}^{(2)}(y, t)}{\partial t} + \frac{\partial X_{0,sw}^{(1)}(y, t)}{\partial y} V_N^{(1)}(X_{0,sw}^{(1)}(y, t), y, t) = U_N^{(2)}(X_{0,sw}^{(2)}(y, t), y, t) \quad (5-b)$$

where superscript “sw” indicates the use of shallow water theory for obtaining the paddle position from the depth-averaged particle velocity at the mean paddle position. One can note that this latter equation has the same form as that of [Zhang et al. \(2007\)](#), except that we respectively treat the first- and second-order solution. As the same manner with [Zhang et al. \(2007\)](#), the final paddle position should be corrected by wave dispersivity,

$$X_0^{(1)}(y, t) = F^{-1} \left[A_1 \cdot F \left[X_{0,sw}^{(1)}(y, t) \right] \right] \quad (6-a)$$

$$X_0^{(2)}(y, t) = F^{-1} \left[A_2 \cdot F \left[X_{0,sw}^{(2)}(y, t) \right] \right] \quad (6-b)$$

where A_1 and A_2 are the first- and second-order coupling coefficients, which can be found in [Yang et al. \(2013\)](#). F and F^{-1} represent the forward and inverse Fourier transform, respectively. Eqs. (6a) and (6b) give the dispersion correction needed when deviating from the shallow water limit.

To solve Eqs. (5a) and (5b), five points Lagrange interpolation method and fourth-order Runge-Kutta scheme are used to smooth the nonlinear distribution of velocity around the moving paddle and treat the time discretization, respectively. Finally, the combined wave paddle position can be given by

$$X_0(y, t) = X_0^{(1)}(y, t) + X_0^{(2)}(y, t) \quad (7)$$

3. Experimental validation and conclusions

To verify the new model, some unidirectional and multidirectional regular waves and irregular wave experiments has so far been tested in a 3D coupled numerical and physical wave basin. OceanWave3D model of Engsig-Karup et al. (2009) was used to simulate the numerical waves. The physical experiments were carried out in the multifunction wave basin of the Dalian University of Technology. The proposed coupling model is applied as the link between the numerical and the physical model. See Fig. 1 for the sketch. Several tests are presented below. In all tests, the numerical model is run beyond the wavemaker to provide the numerical wave information for obtaining the coupling wavemaker signals and comparing the resulting waves. For regular waves, a periodic stream function theory (Fenton, 1988) is applied to provide the depth-averaged velocity. For irregular waves, a standard JONSWAP spectrum was used. Various wave periods and heights are chosen for considering the dimensionless water depth kh and nonlinearity H/L_0 , where L_0 is the wavelength in deep water according to linear theory.

Figure 2 shows regular wave results from the steepest-shallowest (where $H/L_0=0.064$, $kh=0.63$) and deepest water wave cases (where $H/L_0=0.125$, $kh=5.59$), respectively, and compares measured time series of surface elevation at three selected positions (Ref. point 8, 11 and 13, see Figure 1, right panel) in the wave basin, where the wave direction is $\alpha=15^\circ$. On both plots the measurements generally agree with theoretical profiles though some instability can also be found in the left panel of Figure 2.

Figure 3 shows a unidirectional irregular wave case, with the wave direction is 30° and a significant wave height is $H_{m0}=0.12\text{m}$, a peak period of $T_p=1.2\text{s}$, and the relevant shape parameter, $\gamma=3.36$, $\sigma_a=0.07$, $\sigma_b=0.09$. Comparisons of wave profiles are made on the same reference points. Figure 4 shows the similar comparison with that of Figure 3, except that the wave case chosen is multidirectional irregular waves, with the mean wave direction is 30° . A good agreement is observed with the experimental data.

Conclusion from a larger set of experimental data is that the proposed coupled numerical and physical model is generally reliable for deterministically combining 3D wave simulation. Comparisons of the proposed model with the previous method and relevant parametric analysis are not included here for lack of paper space, but will be presented at the Workshop.

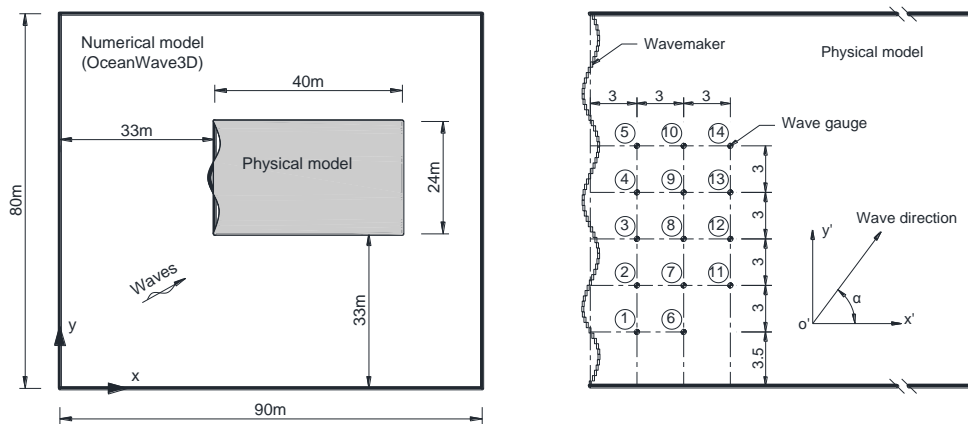


Figure 1. Sketch of the coupled numerical and physical wave basin (left panel), and the layout of the physical basin (right panel).

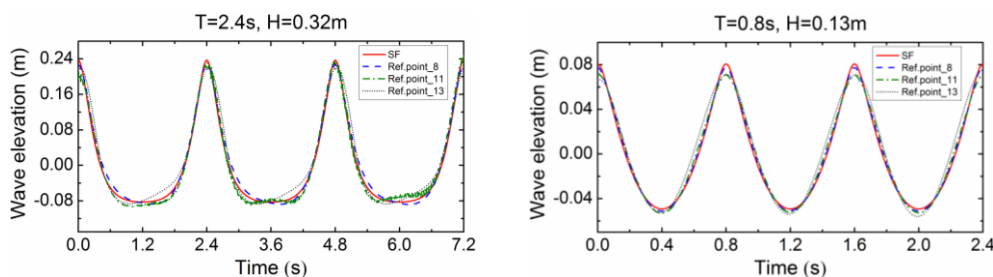


Figure 2. Time series of surface elevations measured at different gauges for unidirectional regular waves, compared with the theoretical stream function theory (SF).

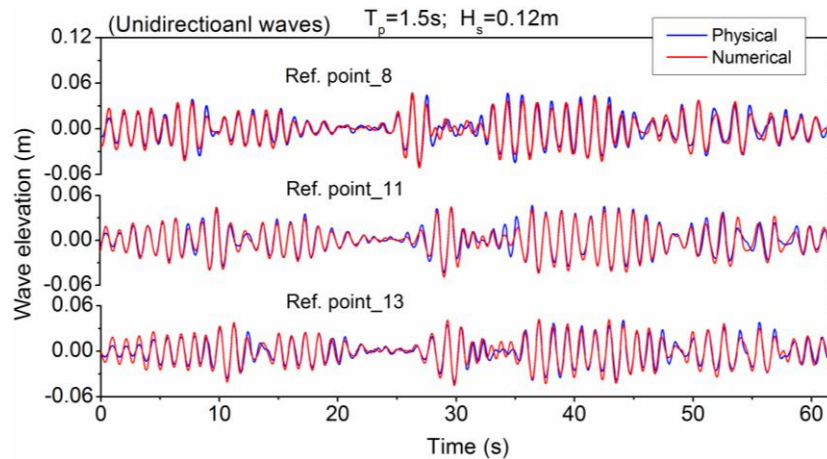


Figure 3. Time series of surface elevations measured at different gauges for unidirectional irregular waves, compared with the numerical results.

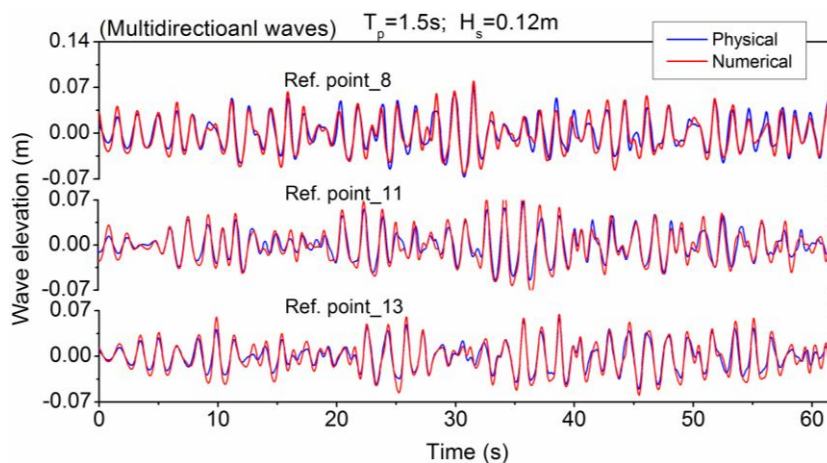


Figure 4. Time series of surface elevations measured at different gauges for multidirectional irregular waves, compared with the numerical results.

References

- Engsig-Karup, A.P., Bingham, H.B., Lindberg, O., 2009. An efficient flexible-order model for 3D nonlinear water waves. *Journal of Computational Physics* 228, 2100–2118.
- Fenton, J.D., 1988. The numerical solution of steady water wave problems. *Computers and Geosciences* 14(3), 357–368.
- Gierlevsen, T., Vargas, B.M., Pires, V.P.L., Acetta, D., 2003. Numerical and physical modelling of storm at Rio Janeiro yacht club. COPEDEC VI, Colombo, Sri Lanka, 15-19 Sept. 2003.
- Kofoed-Hansen, H., Sloth, P., Sørensen, O. R., et al. 2003. Combined numerical and physical modelling of seiche in exposed new marina. *Proceedings of the 27th International Conference on Coastal Engineering*, Sydney, Australia, 2000. 3601-3614.
- Yang, Z., Liu, S., Bingham, H.B., Li, J., 2013. Second-order theory for coupling numerical and physical wave tanks: Derivation, evaluation and experimental validation. *Coastal Engineering* 71, 37-51.
- Zhang, H., Schäffer, H.A., Jakobsen, K.P., 2007. Deterministic combination of numerical and physical coastal wave models. *Coastal Engineering* 54, 171-186.
- Zhang, H., Schäffer, H.A., 2005. Waves in numerical and physical wave basins—a deterministic combination. *Proceedings of Waves 2005*, Madrid, Spain, July, 2005.